Original Article | Neuroimaging and Head & Neck

eISSN 2005-8330
https://doi.org/10.3348/kjr.2022.0299
Korean J Radiol 2022;23(11):1078-1088

Korean Journal of Radiology
KJR

Development and Validation of a Model Using Radiomics Features from an Apparent Diffusion Coefficient Map to Diagnose Local Tumor Recurrence in Patients Treated for Head and Neck Squamous Cell Carcinoma

Minjae Kim[1, 2], Jeong Hyun Lee[1], Leehi Joo[1], Boryeong Jeong[1], Seonok Kim[3], Sungwon Ham[4], Jihye Yun[4], NamKug Kim[4], Sae Rom Chung[1], Young Jun Choi[1], Jung Hwan Baek[1], Ji Ye Lee[5, 6], Ji-hoon Kim[5, 6]

[1]Department of Radiology and Research Institute of Radiology, University of Ulsan College of Medicine, Asan Medical Center, Seoul, Korea; [2]Department of Radiology and Research Institute of Radiological Science and Center for Clinical Imaging Data Science, Yonsei University College of Medicine, Seoul, Korea; [3]Department of Clinical Epidemiology and Biostatistics, University of Ulsan College of Medicine, Asan Medical Center, Seoul, Korea; [4]Department of Convergence Medicine, University of Ulsan College of Medicine, Asan Medical Center, Seoul, Korea; [5]Department of Radiology, Seoul National University Hospital, Seoul, Korea; [6]Department of Radiology, Seoul National University College of Medicine, Seoul, Korea

Objective: To develop and validate a model using radiomics features from apparent diffusion coefficient (ADC) map to diagnose local tumor recurrence in head and neck squamous cell carcinoma (HNSCC).

Materials and Methods: This retrospective study included 285 patients (mean age ± standard deviation, 62 ± 12 years; 220 male, 77.2%), including 215 for training (n = 161) and internal validation (n = 54) and 70 others for external validation, with newly developed contrast-enhancing lesions at the primary cancer site on the surveillance MRI following definitive treatment of HNSCC between January 2014 and October 2019. Of the 215 and 70 patients, 127 and 34, respectively, had local tumor recurrence. Radiomics models using radiomics scores were created separately for T2-weighted imaging (T2WI), contrast-enhanced T1-weighted imaging (CE-T1WI), and ADC maps using non-zero coefficients from the least absolute shrinkage and selection operator in the training set. Receiver operating characteristic (ROC) analysis was used to evaluate the diagnostic performance of each radiomics score and known clinical parameter (age, sex, and clinical stage) in the internal and external validation sets.

Results: Five radiomics features from T2WI, six from CE-T1WI, and nine from ADC maps were selected and used to develop the respective radiomics models. The area under ROC curve (AUROC) of ADC radiomics score was 0.76 (95% confidence interval [CI], 0.62–0.89) and 0.77 (95% CI, 0.65–0.88) in the internal and external validation sets, respectively. These were significantly higher than the AUROC values of T2WI (0.53 [95% CI, 0.40–0.67], $p = 0.006$), CE-T1WI (0.53 [95% CI, 0.40–0.67], $p = 0.012$), and clinical parameters (0.53 [95% CI, 0.39–0.67], $p = 0.021$) in the external validation set.

Conclusion: The radiomics model using ADC maps exhibited higher diagnostic performance than those of the radiomics models using T2WI or CE-T1WI and clinical parameters in the diagnosis of local tumor recurrence in HNSCC following definitive treatment.

Keywords: *Radiomics; Diffusion-weighted imaging; Magnetic resonance imaging; Head and neck squamous cell carcinoma*

Received: May 10, 2022 **Revised:** July 25, 2022 **Accepted:** August 17, 2022

Corresponding author: Jeong Hyun Lee, MD, PhD, Department of Radiology and Research Institute of Radiology, University of Ulsan College of Medicine, Asan Medical Center, 88 Olympic-ro 43-gil, Songpa-gu, Seoul 05505, Korea.
• E-mail: jeonghlee@amc.seoul.kr; and
Ji-hoon Kim, MD, PhD, Department of Radiology, Seoul National University Hospital, 101 Daehak-ro, Jongno-gu, Seoul 03080, Korea.
• E-mail: jihnkim@gmail.com

Korean Journal of Radiology
KJR

INTRODUCTION

Despite recent advances in treatment modalities, local tumor recurrence is the main cause of treatment failure in head and neck squamous cell carcinoma (HNSCC) [1-4]. Accurate and early diagnosis of local tumor recurrence is crucial for the timely implementation of treatment and is heavily dependent on imaging. However, differentiating local tumor recurrence from post-treatment changes is especially challenging, particularly in the era of radiotherapy. Radiation-induced changes may mimic recurrent tumors owing to edema, granulation tissue formation, and fibrosis. Pathological confirmation may be necessary, but should be avoided in heavily irradiated tissue because biopsy procedures may increase the risk of superimposed infection, failure to heal, and edema [5].

The radiomics approach extracts high-dimensional features from routine, standard-of-care imaging data using an automated data-mining algorithm [6,7] and aims to incorporate subsequent analysis and selection of features in clinical decision-making. In HNSCC, studies have demonstrated the diagnostic or prognostic value of radiomics, but studies are limited to applying radiomics to CT and MRI sequences, such as T2-weighted imaging (T2WI) and contrast-enhanced T1-weighted imaging (CE-T1WI) [8,9]. Diffusion-weighted imaging (DWI) is well-established to reflect tumor cellularity, and previous studies have shown that tumor recurrence exhibits a significantly lower apparent diffusion coefficient (ADC) than post-treatment change [10-14]. Moreover, several multicenter studies have demonstrated that ADC maps may show robustness across different acquisition sites and protocols compared with MRI sequences such as T2WI and CE-T1WI, overcoming concerns regarding the generalizability of radiomics models with a potential for applicability in clinical practice [15-17].

We hypothesized that the radiomics approach could be applied to ADC maps to diagnose local tumor recurrence in HNSCC patients. Therefore, this study aimed to develop and validate a model using radiomics features from ADC maps for diagnosing local tumor recurrence in HNSCC and to compare it with radiomics models based on T2WI or T1WI.

MATERIALS AND METHODS

Study Patients

The Institutional Review Boards of Asan Medical Center and Seoul National University Hospital approved this retrospective study, and the requirement for informed consent was waived (IRB No. 2019-1095). We searched the electronic database of the Department of Radiology at two tertiary centers and retrospectively reviewed patient records between January 2014 and October 2019. We identified 366 consecutive patients who met the following inclusion criteria: 1) histopathological diagnosis of HNSCC according to the WHO criteria, 2) completion of a standard treatment regimen for definitive treatment based on the TNM classification according to the 8th edition of the American Joint Committee on Cancer (AJCC) [18], 3) newly developed contrast-enhancing lesions at the primary cancer site on surveillance MRI that included DWI, and 4) diagnosis of local tumor recurrence or post-treatment change on pathologic confirmation or clinico-radiological consensus. Post-treatment imaging findings were used for risk stratification and recommended biopsy consideration with suspicion of tumor recurrence. Local tumor recurrence was diagnosed based on clinico-radiological consensus when definite radiologic or clinical progression was identified with at least 20% increase in maximal diameter. If contrast-enhancing lesions were initially suspected to be post-treatment changes, follow-up imaging studies were performed at 2- to 6-month intervals and subsequently at 1-year intervals. If the contrast-enhancing lesions remained stable or regressed without treatment during a follow-up period of at least 1 year, a post-treatment change was diagnosed. Patients were excluded if 1) the quality of the MRI, including DWI, was inadequate for image analysis (n = 37), and 2) follow-up examinations were inadequate to confidently diagnose tumor recurrence or post-treatment change on clinico-radiological consensus (n = 44). The inclusion and exclusion processes are illustrated in Figure 1. Finally, 215 patients from the Asan Medical Center were included, and a temporal split (3:1) was applied to create an independent validation set. Seventy patients from the Seoul National University Hospital were included in the external validation set.

Imaging Data Acquisition and Processing

All MRI studies at both institutions were performed with a 3T MR imaging scanner (Skyra, Siemens Healthcare; Ingenia, Philips Medical Systems) using a 64- or 20-channel head and neck coil. A detailed description and comparison of the imaging parameters are shown in Supplementary Table 1.

Segmentation of newly appearing contrast-enhancing lesions at the primary cancer site was performed by two neuroradiologists independently (with 7 years of experience

 https://doi.org/10.3348/kjr.2022.0299

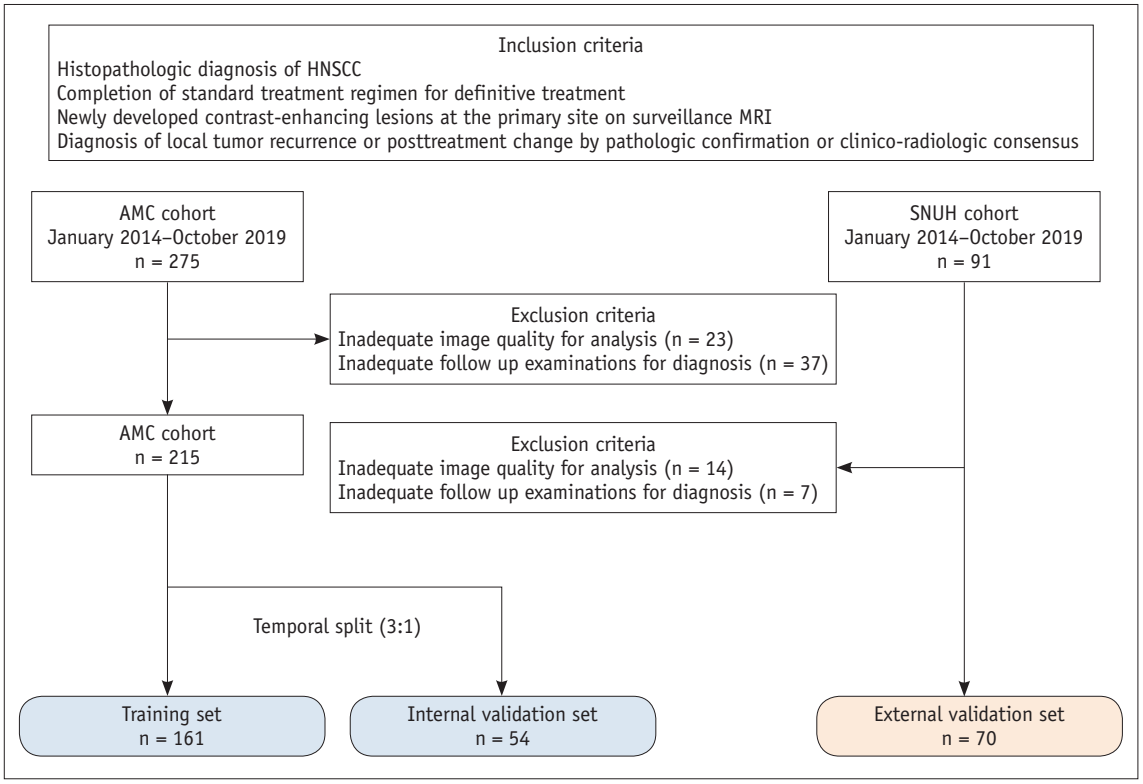

Fig. 1. Flow diagram showing the patient selection protocol and the inclusion and exclusion criteria. AMC = Asan Medical center, HNSCC = head and neck squamous cell carcinoma, SNUH = Seoul National University Hospital

in oncologic imaging for both). The most representative slice of the newly appeared contrast-enhancing lesion was chosen upon reviewing CE-T1WI, T2WI, and DWI, and the region of interest was defined on either CE-T1WI or T2WI, depending on whether the image enabled superior anatomic representation of the lesion. The region of interest was semi-automatically defined using a segmentation threshold and region-growing segmentation algorithm using the MITK software (www.mitk.org, German Cancer Research Center) [19]. All segmented images were validated by an experienced neuroradiologist (with 19 years of experience in oncologic imaging). Finally, we resampled all images into a uniform voxel size of 1 x 1 x 1 mm. T2WI and ADC were then co-registered to the CE-T1WI using the SPM software (www.fil.ion.ucl.ac.uk/spm/). The co-registration process included the generation of a mask from CE-T1WI and transformation of the ADC and T2WI to CE-T1WI using affine transformations with normalized mutual information as a cost function, with 12 degrees of freedom and trilinear interpolation [20].

Radiomics Feature Extraction

Radiomics features were extracted using MATLAB R2014b (MathWorks). For T2WI and CE-T1WI, signal intensity normalization was performed using the ANTsR and Whitestripe packages in R software (R version 3.6.1, https://www.r-project.org) [21,22]. All lesions were included without applying a size cutoff, and the bin number was fixed at 32, which allowed all features to be included without generating spurious results. There were 17 first-order features and 87 texture features. Wavelet transformation was applied to the original images with A, H, V, and D filters to obtain four wavelet-decomposition images, and the first-order and texture features were then applied to the wavelet-transformed images, yielding 416 wavelet-transformed features. This resulted in 520 features from T2WI, CE-T1WI, and ADC per patient. A gray-level co-occurrence matrix (GLCM) was constructed from 2D analysis of the region of interest with 4-connectivity, which was calculated by pixels in each direction and at distances of 1, 2, and 3. The radiomics features used adhered to the standards set by the Imaging Biomarker Standardization Initiative [23]. The code for the feature extraction and analysis pipeline is available in the open repository (https://github.com/jieunp/radiogenomics).

https://doi.org/10.3348/kjr.2022.0299

Korean Journal of Radiology
KJR

Statistical Analysis

Patient Demographics and Clinical Characteristics

The Student's *t* test for continuous variables and the chi-square test or Fisher's exact test for categorical variables were used to assess differences between the training and validation sets regarding the demographic data and the prevalence of each classification category. Statistical significance was set at $p < 0.05$. Statistical analyses were performed using a statistical software (R version 3.6.1).

Selection of Significant Radiomics Features

All radiomics features were normalized by transforming the data into new values with a mean of 0 and standard deviation of 1 (z-score transformation). The concordance correlation coefficient defined by Lin [24] was calculated to account for segmentation variability between two readers, and the features with concordance correlation coefficient > 0.75 (1321/1460, 90.5%) were considered reproducible. The logistic regression analysis to predict local tumor recurrence was performed to calculate area under the receiver operating characteristic (ROC) curve (AUC), and radiomics features with AUC > 0.55 (1042/1321, 78.9%) were pre-selected. Subsequently, to eliminate redundant features, Spearman's correlation coefficient was calculated for all possible feature pairs among 359 features from T2WI, 341 features from CE-T1WI, and 342 features from ADC. For feature pairs demonstrating a Spearman's correlation coefficient > 0.9, the feature with a higher AUC was selected, and the other feature was removed. This resulted in 43 features from T2WI, 34 from CE-T1WI, and 43 from ADC. Then, we applied the least absolute shrinkage and selection operator (LASSO) logistic model to select the significant features with non-zero coefficients [25-28]. To find an optimal λ (the degree of shrinkage), 10-fold cross-validation with minimum criteria was applied, where the final value of λ yielded the minimum cross-validation error.

Individualized Radiomics Score

An individualized radiomics score was developed using the non-zero coefficients of the radiomics features. This score is calculated as the sum of each radiomics feature multiplied by a non-zero coefficient from LASSO, according to the following equation:

Radiomics score = intercept

+ coefficient of the 1st feature x value of the 1st feature

+ coefficient of the 2nd feature x value of the 2nd feature

Table 1. Baseline Demographics and Clinical Characteristics of Patients

	Training Set (n = 161)			Internal Validation Set (n = 54)			External Validation Set (n = 70)		
	Local Tumor Recurrence (n = 91)	Posttreatment Change (n = 70)	*P*	Local Tumor Recurrence (n = 36)	Posttreatment Change (n = 18)	*P*	Local Tumor Recurrence (n = 34)	Posttreatment Change (n = 36)	*P*
Sex, male	70 (76.9)	58 (82.9)	0.351	25 (69.4)	14 (77.8)	0.520	27 (79.4)	26 (72.2)	0.486
Age, years	63 ± 12	63 ± 11	> 0.999	61 ± 12	61 ± 14	0.791	60 ± 14	60 ± 14	> 0.999
Pathologic confirmation	80 (87.9)	14 (20.0)	< 0.001	29 (80.6)	6 (33.3)	< 0.001	12 (35.3)	2 (5.6)	0.002
Clinical stage			0.413			0.323			0.142
I	10 (11.0)	14 (20.0)		5 (13.9)	3 (16.7)		2 (5.9)	8 (22.2)	
II	9 (9.9)	8 (11.4)		7 (19.4)	4 (22.2)		6 (17.6)	9 (25.0)	
III	33 (36.3)	20 (28.6)		9 (25)	8 (44.4)		10 (29.4)	8 (22.2)	
IV	33 (36.3)	26 (37.1)		13 (36.1)	2 (11.1)		11 (32.4)	10 (27.8)	
N/A	6 (6.6)	2 (2.9)		2 (5.6)	1 (5.6)		5 (14.7)	1 (2.8)	
Subsite									
Nasopharynx	15 (16.5)	7 (10.0)	0.236	4 (11.1)	1 (5.6)	0.515	2 (5.9)	1 (2.8)	0.526
Oropharynx	8 (8.8)	12 (17.1)	0.114	4 (11.1)	2 (11.1)	1.000	9 (26.5)	6 (16.7)	0.322
Hypopharynx	2 (2.2)	4 (5.7)	0.246	2 (5.6)	2 (11.1)	0.472	4 (11.8)	4 (11.1)	0.927
Larynx	7 (7.7)	1 (1.4)	0.070	3 (8.3)	1 (5.6)	0.723	2 (5.9)	1 (2.8)	0.526
Oral cavity	39 (42.9)	29 (41.4)	0.849	18 (50.0)	6 (33.3)	0.249	13 (38.2)	17 (47.2)	0.450
Paranasal sinus	20 (22.0)	17 (24.3)	0.732	5 (13.9)	6 (33.3)	0.098	4 (11.8)	7 (19.4)	0.386

Age is expressed as means ± standard deviations. Otherwise, data are number of patients with % in parentheses. N/A = not available

https://doi.org/10.3348/kjr.2022.0299

+ coefficient of the 3rd feature x value of the 3rd feature +...+ coefficient of the nth feature x value of the nth feature

The radiomics score was calculated separately for T2WI, CE-T1WI, ADC, and their combination.

Clinical Parameters

Age, sex, and clinical stage (I–II and III–IV) were considered, and univariable and multivariable logistic regression analyses were performed to diagnose local tumor recurrence in HNSCC.

Model Performance Evaluation

ROC curve analysis was performed to determine the diagnostic performance of the radiomics scores and clinical parameters. The optimal cutoff point of the ROC curve was selected using the highest Youden index [29]. The diagnostic performance of the ADC radiomics score was compared with that of the radiomics scores using T2WI and CE-T1WI and clinical parameters. The diagnostic performance of the combined model incorporating the ADC radiomics score and clinical parameters was also calculated. The AUCs were compared using the Delong test. Statistical significance was set at $p < 0.05$.

RESULTS

Patient Demographics

The baseline demographic and clinical characteristics of the patients are summarized in Table 1. There were 161 patients in the training set (91 with local tumor recurrence and 70 with post-treatment change), 54 in the internal validation set (36 with local tumor recurrence and 18 with post-treatment change), and 70 in the external validation set (34 with local tumor recurrence and 36 with post-treatment change). There were no differences between patients in the development set (training and internal validation sets) and external validation set in age, sex, and clinical stage. Patients were treated according to the standard treatment regimen for definite treatment, including surgery alone (development set vs. external validation set, 25.1% [54/215] vs. 25.7% [18/70], p = 0.920), surgery followed by radiotherapy, chemotherapy, or chemoradiotherapy (45.6% [98/215] vs. 47.1% [33/70], p = 0.827), chemoradiotherapy (19.5% [42/215] vs. 15.7% [11/70], p = 0.478), or radiotherapy alone (9.8% [21/215] vs. 11.4% [8/70], p = 0.701). The mean time interval from the initial diagnosis to the development of contrast-enhancing lesion was 751.9 days (range, 91–3749 days) for the development set and 571.3 days (range, 77–3206 days) for the external validation set (p = 0.131). The diagnosis of local tumor recurrence or post-treatment change was confirmed pathologically in 59.1% (127/215) of the training and internal validation sets and 20.0% (14/70) of the external validation set ($p < 0.001$). There was no difference in the ratio between local tumor recurrence and post-treatment change across all subsites in the training, internal validation, and external validation sets.

Diagnostic Model Using Individualized Radiomics Score

Among 520 radiomics features extracted from T2WI, five were selected to build the individualized T2WI radiomics score. The diagnostic performance of the T2WI radiomics score in the internal validation set was 0.64 (95% confidence interval [CI], 0.47–0.81), with sensitivity of 69.4% (95% CI, 53.1–82.0) and specificity of 55.6% (95% CI, 33.7–75.4). Among the 520 radiomics features extracted from CE-T1WI, six were selected to build the CE-T1WI radiomics score. The diagnostic performance of the CE-T1WI radiomics score in the internal validation set was 0.67 (95% CI, 0.52–0.83), with sensitivity of 83.3% (95% CI,

Table 2. Diagnostic Performance of Radiomics Scores for Diagnosing Local Tumor Recurrence in HNSCC

	Training Set (n = 161)			Internal Validation Set (n = 54)		
	AUC	Sensitivity (%)	Specificity (%)	AUC	Sensitivity (%)	Specificity (%)
ADC score	0.78 (0.71, 0.85)	83.5 (74.6, 89.8)	60.0 (48.3, 70.7)	0.76 (0.63, 0.89)	75.0 (58.9, 86.3)	50.0 (29.0, 71.0)
T2WI score	0.75 (0.67, 0.83)	79.1 (69.7, 86.2)	70.0 (58.5, 79.5)	0.64 (0.47, 0.81)	69.4 (53.1, 82.0)	55.6 (33.7, 75.4)
CE-T1WI score	0.69 (0.61, 0.77)	87.9 (79.6, 93.1)	44.3 (33.2, 55.9)	0.67 (0.52, 0.83)	83.3 (68.1, 92.1)	38.9 (20.3, 61.4)
ADC + T2WI + CE-T1WI score	0.79 (0.72, 0.86)	78.0 (68.5, 85.3)	71.4 (60.0, 80.7)	0.74 (0.60, 0.88)	75.0 (58.9, 86.3)	72.2 (49.1, 87.5)

Numbers in parenthesis are 95% confidence intervals. ADC = apparent diffusion coefficient, AUC = area under the receiver operating characteristic curve, CE-T1WI = contrast-enhanced T1-weighted imaging, HNSCC = head and neck squamous cell carcinoma, T2WI = T2-weighted imaging

https://doi.org/10.3348/kjr.2022.0299

Korean Journal of Radiology
KJR

68.1–92.1) and specificity of 38.9% (95% CI, 20.3–61.4). Among the 520 radiomics features extracted from ADC, 9 features were selected to build the ADC radiomics score. The diagnostic performance of the ADC radiomics score in the internal validation set was 0.76 (95% CI, 0.63–0.89) with sensitivity of 75.0% (95% CI, 58.9–86.3) and specificity of 50.0% (95% CI, 29.0–71.0). Significant features from T2WI, CE-T1WI, and ADC, with correlation coefficients from LASSO, are listed in Supplementary Table 2. The diagnostic performance incorporating the selected features from T2WI, CE-T1WI, and ADC showed an AUC of 0.74 (95% CI, 0.60–0.88) with sensitivity of 75.0% (95% CI, 58.9–86.3) and specificity of 72.2% (95% CI, 49.1–87.5) in the internal validation set. The diagnostic performances of the radiomics scores in the training and internal validation sets are shown in Table 2.

Clinical Parameters

The results of the univariable and multivariable analyses for determining the factors for diagnosing local tumor recurrence using the training set are summarized in Supplementary Table 3. On univariable analysis, age showed an odds ratio (OR) of 1.01 (95% CI, 0.98–1.04; $p = 0.400$), sex showed an OR of 1.1 (95% CI, 0.5–2.6; $p = 0.818$), and clinical stage showed an OR of 1.6 (95% CI, 0.8–3.4; $p = 0.217$). On multivariable analysis, age showed an OR of 1.01 (95% CI, 0.97–1.04; $p = 0.694$), sex showed an OR of 1.7 (95% CI, 0.7–4.6; $p = 0.248$), and clinical stage showed OR of 1.1 (95% CI, 0.5–2.6; $p = 0.837$).

Diagnostic Performance of the Radiomics Scores and Clinical Parameters in the External Validation Set

The diagnostic performance of the radiomics scores and clinical parameters in the external validation sets are shown in Table 3. The AUC of the ADC radiomics score was 0.77 (95% CI, 0.65–0.88), with sensitivity of 97.1% (95% CI, 85.1–99.5) and specificity of 25.0% (95% CI, 13.8–41.1) in the external validation set. This was higher than the T2WI radiomics score with AUC of 0.53 (95% CI, 0.40–0.67; $p = 0.006$), CE-T1WI radiomics score with AUC of 0.53 (95% CI, 0.40–0.67; $p = 0.012$) and clinical parameters with AUC of 0.53 (95% CI, 0.39–0.67; $p = 0.021$). The diagnostic performance of the combined model incorporating the ADC radiomics score and clinical parameters was comparable to the ADC radiomics score with AUC of 0.77 (95% CI, 0.66–0.88; $p = 0.856$). Figures 2 and 3 show representative cases of local tumor recurrence and post-treatment changes,

Table 3. Diagnostic Performance of Radiomics Scores and Clinical Parameters for Diagnosing Local Tumor Recurrence in HNSCC

	Internal Validation Set (n = 54)			External Validation Set (n = 70)			
	AUC	Sensitivity (%)	Specificity (%)	AUC	Sensitivity (%)	Specificity (%)	*P**
Radiomics score							
ADC score	0.76 (0.62, 0.89)	75.0 (58.9, 86.3)	50.0 (29.0, 71.0)	0.77 (0.65, 0.88)	97.1 (85.1, 99.5)	25.0 (13.8, 41.1)	
T2WI score	0.64 (0.47, 0.81)	69.4 (53.1, 82.0)	55.6 (33.7, 75.4)	0.53 (0.40, 0.67)	61.8 (45.0, 76.1)	38.9 (24.8, 55.1)	0.006
CE-T1WI score	0.67 (0.52, 0.83)	83.3 (68.1, 92.1)	38.9 (20.3, 61.4)	0.53 (0.40, 0.67)	100 (89.9, 100)	0 (0, 9.6)	0.012
ADC + T2WI + CE-T1WI score	0.74 (0.60, 0.88)	75.0 (58.9, 86.3)	55.6 (33.7, 75.4)	0.74 (0.63, 0.86)	85.3 (69.9, 93.6)	38.9 (24.8, 55.1)	0.435
Clinical parameters (age, sex, clinical stage)	0.55 (0.39, 0.71)	41.7 (27.1, 57.8)	61.1 (38.6, 79.7)	0.53 (0.39, 0.67)	29.4 (16.8, 46.2)	77.8 (61.9, 88.3)	0.021
Combined model (ADC score + clinical parameters)	0.77 (0.64, 0.91)	47.2 (32.0, 63.0)	94.4 (74.2, 99.0)	0.77 (0.66, 0.88)	82.4 (66.5, 91.7)	52.8 (37.0, 68.0)	0.856

Numbers in parenthesis are 95% confidence intervals. *p value for the comparison of AUC in reference to the AUC of ADC radiomics score. ADC = apparent diffusion coefficient, AUC = area under the receiver operating characteristic curve, CE-T1WI = contrast-enhanced T1-weighted imaging, HNSCC = head and neck squamous cell carcinoma, T2WI = T2-weighted imaging

https://doi.org/10.3348/kjr.2022.0299

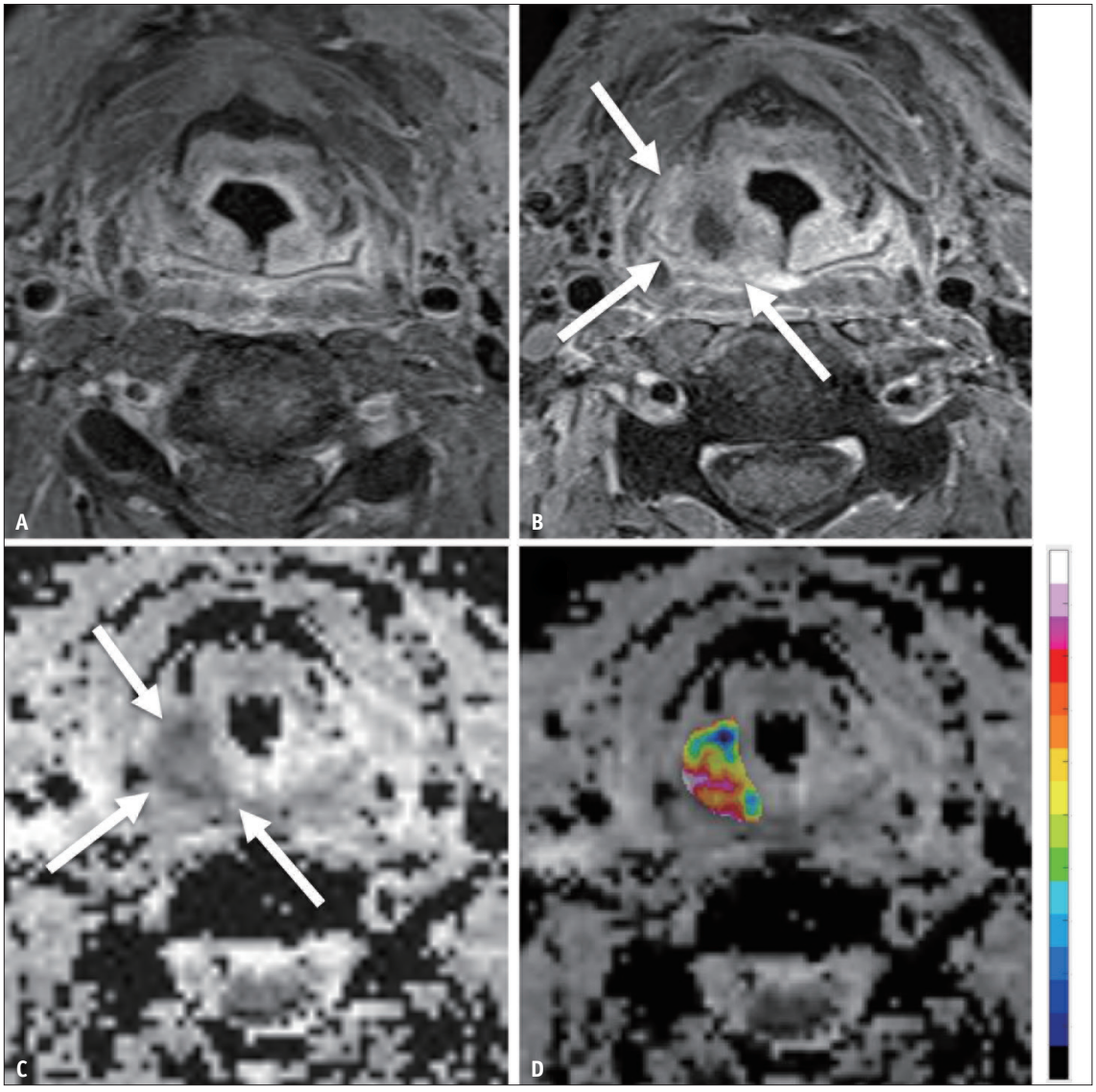

Fig. 2. A 55-year-old male treated by concurrent chemoradiotherapy for right hypopharyngeal squamous cell carcinoma (T4aN2bM0, clinical stage IVA).
A. Contrast-enhanced T1-weighted image after the completion of concurrent chemoradiotherapy shows complete remission. **B.** During surveillance, contrast-enhanced T1-weighted image shows newly developed, ill-defined contrast-enhancing mass at the right pyriform sinus (arrows). **C.** Mean ADC value of the enhancing lesion (arrows) was 0.92 mm^2/s (standard deviation = 0.12 mm^2/s) on the ADC map. **D.** A voxel-based color-scaled map of a representative significant ADC radiomics feature overlayed on the ADC map demonstrates high entropy. The mass was confirmed to be recurrent squamous cell carcinoma on excision. ADC = apparent diffusion coefficient

respectively.

DISCUSSION

To our knowledge, this was the first study to develop and validate a model using radiomics features from ADC maps to diagnose local tumor recurrence in HNSCC patients after definitive treatment. We constructed individualized radiomics scores from the significant radiomics features extracted from T2WI, CE-T1WI, and ADC images using non-zero coefficients from LASSO. The ADC radiomics score showed a higher diagnostic performance than T2WI or CE-T1WI and clinical parameters. Moreover, the diagnostic performance of the ADC radiomics score in the external validation set was comparable to that in the internal validation set. This underscores the potential and generalizability of the ADC radiomics score for the diagnosis of local tumor recurrence in HNSCC in clinical practice.

Previous studies have shown that recurrent tumors can be differentiated from post-treatment changes based on

https://doi.org/10.3348/kjr.2022.0299

Korean Journal of Radiology
KJR

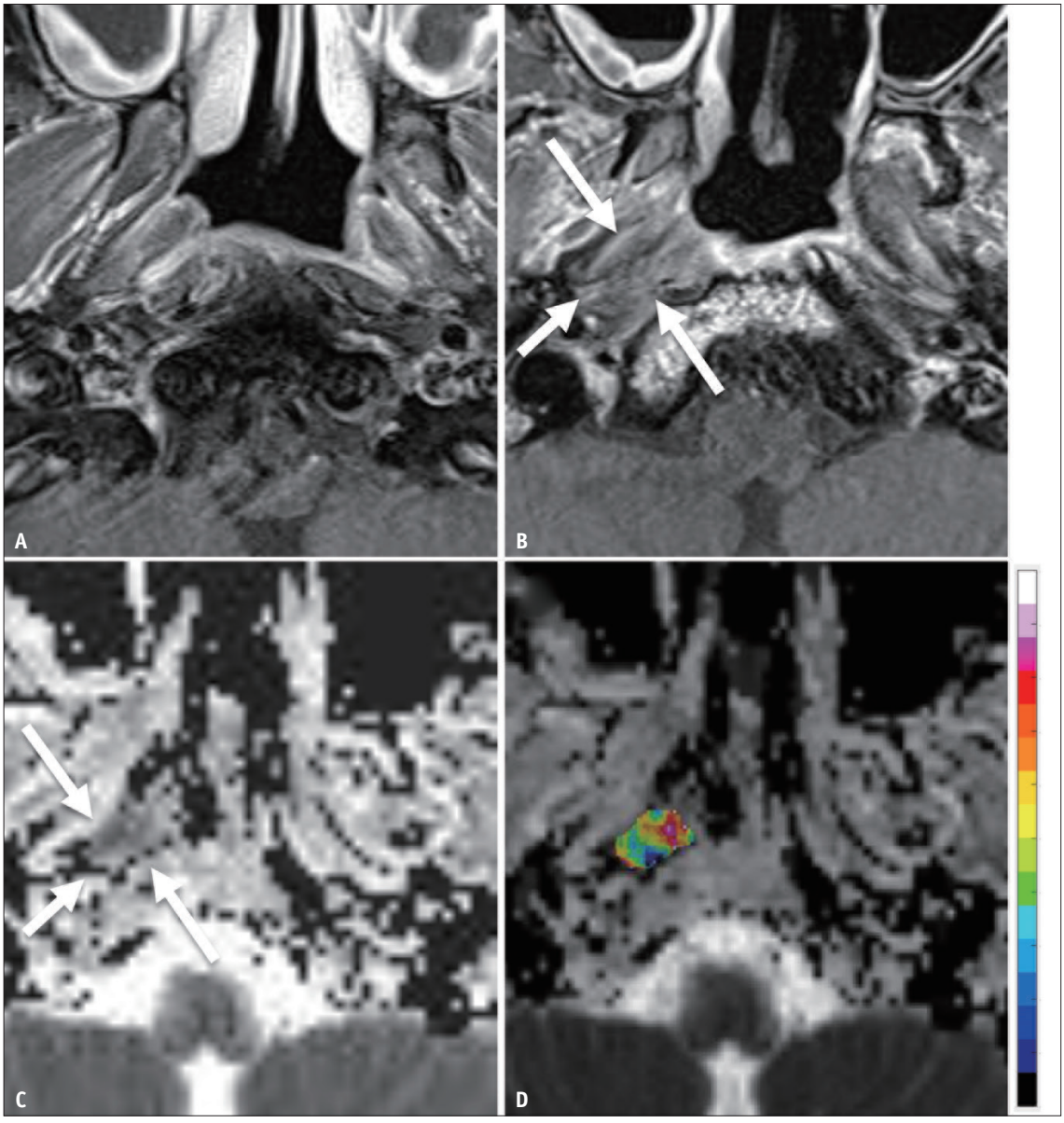

Fig. 3. A 38-year-old male treated by concurrent chemoradiotherapy for non-keratinizing carcinoma of the nasopharynx (T3N1M0, clinical stage III).
A. Contrast-enhanced T1-weighted image after the completion of concurrent chemoradiotherapy shows complete remission. **B.** During surveillance, contrast-enhanced T1-weighted image demonstrates newly developed contrast-enhancing mass at the right side of the nasopharynx (arrows). **C.** The mass shows low ADC value (arrows) with mean ADC of 0.86 mm^2/s (standard deviation = 0.22 mm^2/s) on the ADC map raising suspicion of local tumor recurrence. **D.** A voxel-based color-scaled map of a representative significant ADC radiomics feature overlayed on the ADC map demonstrates low entropy. Excisional biopsy was performed and revealed inflamed granulation tissue. ADC = apparent diffusion coefficient

ADC values, with sensitivity of 69%–100% and specificity of 77%–95% [10-14]. Significantly lower ADC values have been observed in recurrent tumors, which reflects their hypercellularity [30,31], whereas post-treatment changes exhibited relatively low cellularity associated with variable degrees of edema and inflammatory reaction. Previous studies regarding radiomics analysis of MR images utilized T2WI and CE-T1WI and reported diagnostic performance with an AUC of up to 0.85 for preoperative discrimination of clinical stage or for determination of human papillomavirus (HPV) infection status [32,33]. A limited number of studies have explored radiomics approaches using ADC maps, none of which have evaluated ADC radiomics to diagnose local tumor recurrence in HNSCC [34,35]. In our study, we were able to tease out the higher performance of the diagnostic model using ADC maps compared to the models using T2WI

 https://doi.org/10.3348/kjr.2022.0299

and CE-T1WI, which were externally validated.

Combining the selected radiomics features from ADC, T2WI, and CE-T1WI did not improve the diagnostic performance of the ADC radiomics score alone. Additionally, combining clinical parameters with the ADC radiomics score did not improve the diagnostic performance of the ADC radiomics score. These results suggest that the ADC radiomics score may provide a unique value that is not achievable by radiomics scores using T2WI and CE-T1WI. Significant ADC radiomics features included minimum ADC and variance, which may indicate that not only high cellularity but also the degree of heterogeneity plays an important role. Furthermore, the most relevant feature among the selected descriptors was derived from the GLCM. GLCM is a texture-analysis method that calculates how often pairs of pixels with specific values and in a specified spatial relationship occur in an image, and reflects the heterogeneity of tumors [36]. The radiomic approach may offer improved discriminatory power by demonstrating voxel-based heterogeneity using various methods.

In terms of diagnostic performance, the ADC radiomics score demonstrated very high sensitivity (97.1%) but low specificity (25%). This indicates that this tool should be used in conjunction with other parameters to improve the specificity. In this study, HPV status was considered when establishing clinical stages in cases of oropharyngeal cancer when available, although HPV status was largely unavailable, especially before to the 8th edition of the AJCC. Clinical parameters, including extranodal extension and perineural invasion, which are established risk factors for local tumor recurrence, should be considered. Given its high sensitivity, the ADC radiomics score may be utilized as a supplementary tool to improve radiologists' diagnostic performance or workflow, which needs further validation for incorporation in clinical practice.

The lack of standardization of acquisition protocols has often been an obstacle that prevents the use of radiomics models as biomarkers in multicenter practices. However, the strength of our study is that diagnostic models using radiomics features were validated using an external cohort obtained under heterogeneous acquisition protocols. The ADC radiomics score maintained comparable diagnostic performance among the training, internal validation, and external validation sets, whereas the diagnostic performance decreased with the radiomics scores using T2WI and CE-T1WI in the external validation set. The parametric nature of ADC maps obviates the need for signal normalization, unlike T2WI or CE-T1WI, which may contribute to their robustness across different acquisition schemes with a potential for generalizability and applicability in clinical practice.

Our study had some limitations owing to its retrospective nature. All patients were staged according to the 8th edition of the AJCC, and patients diagnosed prior to its availability were restaged accordingly. However, patients staged and treated according to the prior edition of the AJCC were likely to have undergone different treatment regimens, particularly in cases of oropharyngeal cancer with recognition and reflection of HPV or p16 positivity in clinical staging. This accounted for 11.6% of patients in the development set and 21.4% in the external validation set. Additionally, HNSCC patients with heterogeneous primary cancer sites who underwent different treatment modalities and regimens according to the primary cancer site were included, which might have partly accounted for the clinical stage not being identified as a significant factor in diagnosing local tumor recurrence on logistic regression analyses. Moreover, radiomics features were extracted from a single representative image of newly appearing contrast-enhancing lesions, and volume-based radiomics analysis is warranted to validate the findings of our study further.

In conclusion, the diagnostic model using radiomics features from ADC maps showed a higher performance than radiomics models using T2WI or CE-T1WI and clinical parameters in the diagnosis of local tumor recurrence in HNSCC following definitive treatment. These results suggest the potential of the model using radiomics features from the ADC map as a biomarker for diagnosing local tumor recurrence in HNSCC.

Supplement

The Supplement is available with this article at https://doi.org/10.3348/kjr.2022.0299.

Availability of Data and Material

The datasets generated or analyzed during the study are available from the corresponding author on reasonable request.

Conflicts of Interest

Jeong Hyun Lee, NamKug Kim, Jung Hwan Baek, and Ji-hoon Kim who is on the editorial board of the *Korean Journal of Radiology* was not involved in the editorial

Korean Journal of Radiology
KJR

evaluation or decision to publish this article. All remaining authors have declared no conflicts of interest.
Jung Hwan Baek's financial activities are not related to the present article; he has been a consultant to two radiofrequency companies, STARmed and RF Medical, since 2017.

Author Contributions

Conceptualization: Minjae Kim, Jeong Hyun Lee, Ji-hoon Kim, NamKug Kim. Data curation: Leehi Joo, Boryeong Jeong, Sae Rom Chung, Young Jun Choi, Jung Hwan Baek, Ji Ye Lee, Ji-hoon Kim. Formal analysis: Seonok Kim, Sungwon Ham, Jihye Yun. Investigation: Seonok Kim, Sungwon Ham, Jihye Yun. Methodology: Seonok Kim, Sungwon Ham, Jihye Yun, NamKug Kim. Project administration: Jeong Hyun Lee, Ji-hoon Kim. Resources: Jeong Hyun Lee, Ji-hoon Kim, Sungwon Ham, Jihye Yun, NamKug Kim. Software: Sungwon Ham, Jihye Yun, NamKug Kim. Supervision: Jeong Hyun Lee, Ji-hoon Kim. Validation: Jeong Hyun Lee, Ji-hoon Kim. Visualization: Minjae Kim, Jeong Hyun Lee, Ji-hoon Kim, NamKug Kim. Writing—original draft: Minjae Kim, Jeong Hyun Lee, Ji-hoon Kim. Writing—review & editing: all authors.

ORCID iDs

Minjae Kim
https://orcid.org/0000-0002-5382-9360
Jeong Hyun Lee
https://orcid.org/0000-0002-0021-4477
Leehi Joo
https://orcid.org/0000-0002-5527-0476
Boryeong Jeong
https://orcid.org/0000-0003-2664-0252
Seonok Kim
https://orcid.org/0000-0001-9010-5460
Sungwon Ham
https://orcid.org/0000-0002-2886-6952
Jihye Yun
https://orcid.org/0000-0002-5233-6687
NamKug Kim
https://orcid.org/0000-0002-3438-2217
Sae Rom Chung
https://orcid.org/0000-0003-4219-7166
Young Jun Choi
https://orcid.org/0000-0001-7098-5042
Jung Hwan Baek
https://orcid.org/0000-0003-0480-4754
Ji Ye Lee
https://orcid.org/0000-0002-3929-6254
Ji-hoon Kim
https://orcid.org/0000-0002-6349-6950

Funding Statement

None

REFERENCES

1. Agra IM, Carvalho AL, Ulbrich FS, de Campos OD, Martins EP, Magrin J, et al. Prognostic factors in salvage surgery for recurrent oral and oropharyngeal cancer. *Head Neck* 2006;28:107-113
2. Goodwin WJ Jr. Salvage surgery for patients with recurrent squamous cell carcinoma of the upper aerodigestive tract: when do the ends justify the means? *Laryngoscope* 2000;110(3 Pt 2 Suppl 93):1-18
3. Kowalski LP, Bagietto R, Lara JR, Santos RL, Silva JF Jr, Magrin J. Prognostic significance of the distribution of neck node metastasis from oral carcinoma. *Head Neck* 2000;22:207-214
4. Carvalho AL, Magrin J, Kowalski LP. Sites of recurrence in oral and oropharyngeal cancers according to the treatment approach. *Oral Dis* 2003;9:112-118
5. Bahadur S, Amatya RC, Kacker SK. The enigma of post-radiation oedema and residual or recurrent carcinoma of the larynx and pyriform fossa. *J Laryngol Otol* 1985;99:763-765
6. Aerts HJ, Velazquez ER, Leijenaar RT, Parmar C, Grossmann P, Carvalho S, et al. Decoding tumour phenotype by noninvasive imaging using a quantitative radiomics approach. *Nat Commun* 2014;5:4006
7. Kumar V, Gu Y, Basu S, Berglund A, Eschrich SA, Schabath MB, et al. Radiomics: the process and the challenges. *Magn Reson Imaging* 2012;30:1234-1248
8. Wong AJ, Kanwar A, Mohamed AS, Fuller CD. Radiomics in head and neck cancer: from exploration to application. *Transl Cancer Res* 2016;5:371-382
9. Giraud P, Giraud P, Gasnier A, El Ayachy R, Kreps S, Foy JP, et al. Radiomics and machine learning for radiotherapy in head and neck cancers. *Front Oncol* 2019;9:174
10. Jajodia A, Aggarwal D, Chaturvedi AK, Rao A, Mahawar V, Gairola M, et al. Value of diffusion MR imaging in differentiation of recurrent head and neck malignancies from post treatment changes. *Oral Oncol* 2019;96:89-96
11. Driessen JP, Caldas-Magalhaes J, Janssen LM, Pameijer FA, Kooij N, Terhaard CH, et al. Diffusion-weighted MR imaging in laryngeal and hypopharyngeal carcinoma: association between apparent diffusion coefficient and histologic findings. *Radiology* 2014;272:456-463
12. Vaid S, Chandorkar A, Atre A, Shah D, Vaid N. Differentiating recurrent tumours from post-treatment changes in head and neck cancers: does diffusion-weighted MRI solve the eternal

dilemma? *Clin Radiol* 2017;72:74-83
13. Desouky S, AboSeif S, Shama S, Gaafar A, Gamaleldin O. Role of dynamic contrast enhanced and diffusion weighted MRI in the differentiation between post treatment changes and recurrent laryngeal cancers. *Egypt J Radiol Nucl Med* 2015;46:379-389
14. Vandecaveye V, De Keyzer F, Nuyts S, Deraedt K, Dirix P, Hamaekers P, et al. Detection of head and neck squamous cell carcinoma with diffusion weighted MRI after (chemo) radiotherapy: correlation between radiologic and histopathologic findings. *Int J Radiat Oncol Biol Phys* 2007;67:960-971
15. Park JE, Park SY, Kim HJ, Kim HS. Reproducibility and generalizability in radiomics modeling: possible strategies in radiologic and statistical perspectives. *Korean J Radiol* 2019;20:1124-1137
16. Kang D, Park JE, Kim YH, Kim JH, Oh JY, Kim J, et al. Diffusion radiomics as a diagnostic model for atypical manifestation of primary central nervous system lymphoma: development and multicenter external validation. *Neuro Oncol* 2018;20:1251-1261
17. Kim JY, Park JE, Jo Y, Shim WH, Nam SJ, Kim JH, et al. Incorporating diffusion- and perfusion-weighted MRI into a radiomics model improves diagnostic performance for pseudoprogression in glioblastoma patients. *Neuro Oncol* 2019;21:404-414
18. Amin MB, Greene FL, Edge SB, Compton CC, Gershenwald JE, Brookland RK, et al. The eighth edition AJCC cancer staging manual: continuing to build a bridge from a population-based to a more "personalized" approach to cancer staging. *CA Cancer J Clin* 2017;67:93-99
19. Nolden M, Zelzer S, Seitel A, Wald D, Müller M, Franz AM, et al. The medical imaging interaction toolkit: challenges and advances. *Int J Comput Assist Radiol Surg* 2013;8:607-620
20. Maes F, Collignon A, Vandermeulen D, Marchal G, Suetens P. Multimodality image registration by maximization of mutual information. *IEEE Trans Med Imaging* 1997;16:187-198
21. Avants BB, Tustison NJ, Song G, Cook PA, Klein A, Gee JC. A reproducible evaluation of ANTs similarity metric performance in brain image registration. *Neuroimage* 2011;54:2033-2044
22. Shinohara RT, Sweeney EM, Goldsmith J, Shiee N, Mateen FJ, Calabresi PA, et al. Statistical normalization techniques for magnetic resonance imaging. *Neuroimage Clin* 2014;6:9-19
23. Zwanenburg A, Vallières M, Abdalah MA, Aerts HJWL, Andrearczyk V, Apte A, et al. The image biomarker standardization initiative: standardized quantitative radiomics for high-throughput image-based phenotyping. *Radiology* 2020;295:328-338
24. Lin LI. A concordance correlation coefficient to evaluate reproducibility. *Biometrics* 1989;45:255-268
25. Hepp T, Schmid M, Gefeller O, Waldmann E, Mayr A. Approaches to regularized regression–a comparison between gradient boosting and the lasso. *Methods Inf Med* 2016;55:422-430
26. Gui J, Li H. Penalized cox regression analysis in the high-dimensional and low-sample size settings, with applications to microarray gene expression data. *Bioinformatics* 2005;21:3001-3008
27. Wu TT, Chen YF, Hastie T, Sobel E, Lange K. Genome-wide association analysis by lasso penalized logistic regression. *Bioinformatics* 2009;25:714-721
28. Tibshirani R. Regression shrinkage and selection via the lasso. *J R Stat Soc Ser B Methodol* 1996;58:267-288
29. Youden WJ. Index for rating diagnostic tests. *Cancer* 1950;3:32-35
30. Surov A, Stumpp P, Meyer HJ, Gawlitza M, Höhn AK, Boehm A, et al. Simultaneous (18)F-FDG-PET/MRI: associations between diffusion, glucose metabolism and histopathological parameters in patients with head and neck squamous cell carcinoma. *Oral Oncol* 2016;58:14-20
31. Swartz JE, Driessen JP, van Kempen PMW, de Bree R, Janssen LM, Pameijer FA, et al. Influence of tumor and microenvironment characteristics on diffusion-weighted imaging in oropharyngeal carcinoma: a pilot study. *Oral Oncol* 2018;77:9-15
32. Ren J, Tian J, Yuan Y, Dong D, Li X, Shi Y, et al. Magnetic resonance imaging based radiomics signature for the preoperative discrimination of stage I-II and III-IV head and neck squamous cell carcinoma. *Eur J Radiol* 2018;106:1-6
33. Suh CH, Lee KH, Choi YJ, Chung SR, Baek JH, Lee JH, et al. Oropharyngeal squamous cell carcinoma: radiomic machine-learning classifiers from multiparametric MR images for determination of HPV infection status. *Sci Rep* 2020;10:17525
34. Fujima N, Shimizu Y, Yoshida D, Kano S, Mizumachi T, Homma A, et al. Machine-learning-based prediction of treatment outcomes using MR imaging-derived quantitative tumor information in patients with sinonasal squamous cell carcinomas: a preliminary study. *Cancers (Basel)* 2019;11:800
35. Zhang L, Zhou H, Gu D, Tian J, Zhang B, Dong D, et al. Radiomic nomogram: pretreatment evaluation of local recurrence in nasopharyngeal carcinoma based on MR imaging. *J Cancer* 2019;10:4217-4225
36. Haralick RM, Shanmugam K, Dinstein IH. Textural features for image classification. *IEEE Trans Syst Man Cybern* 1973;SMC-3:610-621

https://doi.org/10.3348/kjr.2022.0299